High-spin intruder states in the mirror nuclei ^{31}S and ^{31}P

D. A. Testov,[1,2,3,*] A. Boso,[1,2] S. M. Lenzi,[1,2] F. Nowacki,[4] F. Recchia,[1,2] G. de Angelis,[5] D. Bazzacco,[2] G. Colucci,[1,2,6] M. Cottini,[1] F. Galtarossa,[5] A. Goasduff,[1,2] A. Gozzelino,[5] K. Hadyńska-Klęk,[5,6] G. Jaworski,[5,6] P. R. John,[7] S. Lunardi,[1,2] R. Menegazzo,[2] D. Mengoni,[1,2] A. Mentana,[8] V. Modamio,[9] A. Nannini,[10,11] D. R. Napoli,[5] M. Palacz,[6] M. Rocchini,[10,11,†] M. Siciliano,[5,12,‡] and J. J. Valiente-Dobón[5]

[1]*Dipartimento di Fisica e Astronomia dell'Università di Padova, Padova 35131, Italy*
[2]*INFN, Sezione di Padova, Padova 35131, Italy*
[3]*Joint Institute for Nuclear Research, Dubna, Moscow region, 141980, Russia*
[4]*Institut Pluridisciplinaire Hubert CURIEN (IPHC), Strasbourg 67200, France*
[5]*INFN, Laboratori Nazionali di Legnaro, Legnaro 35020, Italy*
[6]*Heavy Ion Laboratory, University of Warsaw, Warsaw, 02-093, Poland*
[7]*Institut für Kernphysik, Technische Universität Darmstadt, Darmstadt 64289, Germany*
[8]*Dipartimento di Fisica dell'Università di Milano and INFN, Sezione di Milano, Milano 20133, Italy*
[9]*University of Oslo, Oslo 0316, Norway*
[10]*Università degli Studi di Firenze, Florence 50121, Italy*
[11]*INFN, Sezione di Firenze, Florence 50019, Italy*
[12]*IRFU/CEA, Universitè de Paris-Saclay, Gif-sur-Yvette 91191, France*

(Received 17 November 2020; revised 27 December 2020; accepted 1 June 2021; published 5 August 2021)

Mirror energy differences (MED) between excited states in the $A = 31$, $T = 1/2$ mirror pair ^{31}S and ^{31}P have been measured up to high spin yrast states of positive and negative parity. The mirror nuclei were populated in the ^{24}Mg(^{12}C, αn) and ^{24}Mg(^{12}C, αp) reactions, respectively. For the first time the MED are described in the framework of the shell model in a valence space that includes three main shells. The theoretical MED values as a function of angular momentum indicate that the main contribution arises from the Coulomb interaction, however, the isospin symmetry breaking term is not at all negligible and needs to be considered to reproduce the experimental findings.

DOI: 10.1103/PhysRevC.104.024309

I. INTRODUCTION

Nuclei located at or close to the $N = Z$ line are the only region in the Chart of Nuclides where it is possible to find answers to some fundamental problems in nuclear physics, such as the isospin symmetry of the nuclear interaction. One of the consequences of this symmetry is that the level schemes of mirror nuclei (obtained by interchanging the number of neutrons and protons) should be identical. The differences between the excitation energy of analog states, called mirror energy differences (MED), are, therefore, an important signature of the isospin symmetry breaking. Although the Coulomb interaction is the main responsible of this asymmetry, it has been pointed out that isospin symmetry breaking (ISB) terms could arise from the residual nuclear interaction [1].

Interestingly, the behavior of the MED, as a function of the angular momentum, strongly depends on the structural changes of the nuclei and therefore the MED have been deployed as a tool to understand the evolution of the nuclear structure properties with the increasing angular momentum [2,3]. These studies have been mainly concentrated in nuclei of the $f_{7/2}$ shell, where the MED have been measured up to high spins. Nuclei in the *sd* shell are hard to be populated at high spins, in particular, in the proton-rich side, as they soon become proton unbound. Only for a reduced number of nuclei, near to the $N = Z$ line, which presents a sizable degree of deformation, relatively high spin states can be populated. In a recent work [4] MED in the $T = 1/2$ pair ^{23}Mg - ^{23}Na were reported. The authors show that the MED can not only give information on the nuclear structure changes as a function of the angular momentum, but can be also used to provide information on the nuclear skin.

Above ^{28}Si nuclei gain angular momentum and collectivity by particle-hole excitations to the upper *fp* shell. These intruder states appear already at relatively low excitation energy [5,6]. In this context, the mirror pair ^{31}S - ^{31}P constitutes an interesting case. A previous study performed with Gammasphere [7] has reported yrast states of both positive and negative parity that exhibit a sizable degree of collectivity.

*Present address: Extreme Light Infrastructure - Nuclear Physics, IFIN-HH, Bucharest-Magurele, 077125, Romania.
†Present address: University of Guelph, Department of Physics, N1G2W1 Guelph, Canada.
‡Present address: Physics Department, Argonne National Laboratory, Lemont-IL, 60439, USA.

More recently, Doherty and collaborators [8] have performed an extensive study of the low-spin structure of these mirror nuclei for astrophysical applications. They interpret the MED only for the positive-parity states in the shell-model framework and stress the necessity of relying on a good theoretical description of the MED to allow theoretical estimates in situations where experimental data are unavailable. The structure of ^{31}S is of astrophysical interest because it lies at a potential bottleneck for nova nucleosynthesis through the ^{30}P$(p,\gamma)^{31}$S reaction, responsible for the abundance of elements with mass larger than $A = 30$ in classical novae. With the goal of looking at states in ^{31}S relevant for this process, reactions induced by light ions have been studied in Ref. [9]. More recently, low-spin excited states in ^{31}S, populated in β decay, have been reported and compared with different improved versions of the usb interaction [10]. The authors underline the importance of having a good theoretical description of the structure of this nucleus to help the assignment of spin and parity to resonant states that might affect the production rate in proton capture reactions.

In this work we report on an experimental study of excited states in ^{31}S and ^{31}P and describe, for the first time, the MED for both positive- and negative-parity states using the same effective interaction in a large model space. Experimental details are reported in Sec. II while the results for the level schemes of ^{31}P and ^{31}S are given in Secs. III and IV, respectively. The theoretical interpretation of the MED is discussed in Sec. V. Finally, conclusions are drawn in Sec. VI.

II. EXPERIMENTAL DETAILS

The ^{31}S and ^{31}P nuclei were populated via the ^{24}Mg(^{12}C, $1\alpha 1n$) and ^{24}Mg(^{12}C, $1\alpha 1p$) reactions, respectively, using a 45 MeV ^{12}C beam delivered by the XTU-Tandem accelerator of the Legnaro National Laboratories impinging on a 400 μg/cm^2-thick ^{24}Mg self-supported target. Coincident γ rays were detected using the GALILEO array [11] comprising 25 Compton-suppressed HPGe tapered detectors, originally from GASP [12]. Detectors were arranged in three angular groups at 152°, 129°, 119° containing five detectors each plus ten detectors placed at 90° with respect to the beam direction. Events were collected when at least two HPGe detectors fired in coincidence. Efficiency and energy calibration was done using standard sources of ^{60}Co and ^{152}Eu. The channel selection was performed using the EUCLIDES Si-ball light charged-particle array [13,14] and the Neutron Wall [15,16].

In the off-line analysis E_γ-E_γ matrices were incremented in coincidence with $1\alpha 1p$ or $1\alpha 1n$ to select ^{31}P and ^{31}S, respectively. Data from EUCLIDES were also used for the kinematical reconstruction of every event in order to perform the correction for the Doppler effect on an event-by-event basis. The resolving power of the GALILEO array coupled to the ancillary detectors (EUCLIDES and Neutron Wall) is illustrated in Fig. 1 in which γ-ray spectra recorded using the $1\alpha 1p$ or $1\alpha 1n$ particle condition and gating on the $\frac{3}{2}^+ \rightarrow \frac{1}{2}^+$ transition of 1249 keV in ^{31}S and 1266 keV ^{31}P are shown.

To determine the multipolarity of the transitions in order to assign spin and parity to the different levels we have measured

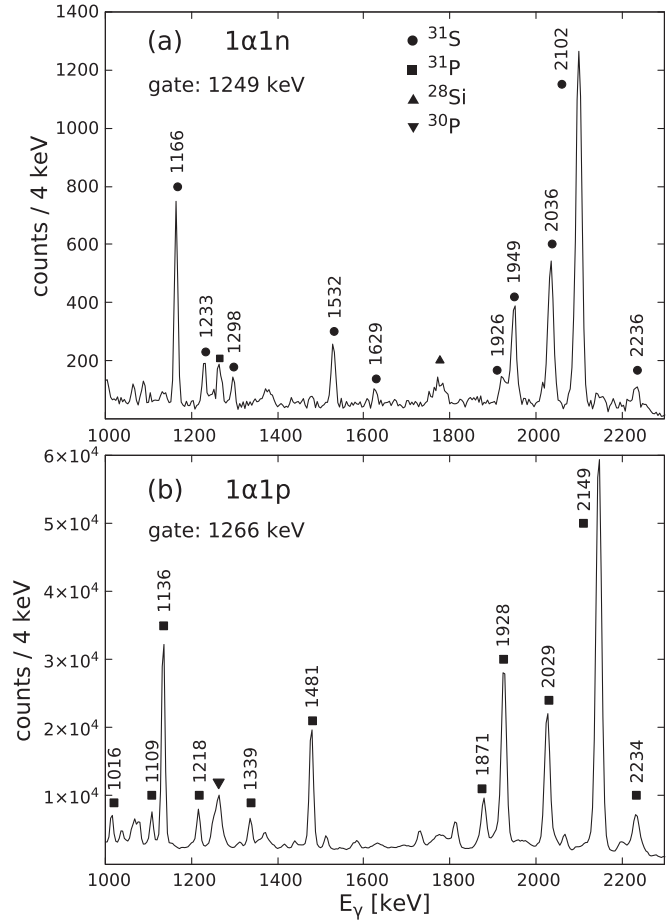

FIG. 1. Background-subtracted coincidence spectra obtained from E_γ-E_γ matrix using (a) $1\alpha 1n$ or (b) $1\alpha 1p$ condition and with a gate on the $3/2^+ \rightarrow 1/2^+$ γ-ray transition.

the angular distributions from oriented states (ADO) ratios [17]. For this purpose two additional E_γ-E_γ matrices were produced having on the first axis γ-ray energy detected by detectors in the ring 90° or 152°, respectively, and on the second axis by all the other detectors. The $R_{\rm ADO}$ is obtained as:

$$R_{\rm ADO} = \frac{I_\gamma(152^\circ)}{I_\gamma(90^\circ)}. \quad (1)$$

At the present GALILEO configuration the angular distribution ratios have values $R_{ADO} \approx 0.64$ and $R_{ADO} \approx 1.4$ for stretched dipole and stretched quadrupole transitions, respectively. For nonstretched dipole transitions a ratio similar to the stretched quadrupole ones is expected. In case of mixed multipolarity R_{ADO} depends on the value and the sign of the mixing coefficient.

III. LEVEL SCHEME OF ^{31}P

The level scheme of ^{31}P is well known as reported in Refs. [7,18]. Using the reaction ^{12}C(^{20}Ne, p) Jenkins and collaborators [7] populated states in ^{31}P up to a level at 12171 keV, tentatively assigned as $(15/2^+)$. Ionescu-Bujor

TABLE I. Transition energies for the observed γ rays in ^{31}P along with the energy for the initial and final states, angular distribution ratio, multipolarity, and relative intensity. Whenever angular distribution ratio were not measured in the present work, multipolarities were assigned in agreement with Ref. [18].

E_γ	E_i	E_f					
	keV		R_{ADO}	I_i	I_f	Mult.	I_γ^{rel}
987.0(4)	7442	6454		$11/2^+$	$11/2^+$	M1+E2	
1016.5(5)	4431	3415	1.16(13)	$7/2^-$	$7/2^+$	$E1$	
1061.9(5)	3295	2234	1.21(9)	$5/2^+$	$5/2^+$	$M1+E2$	80(21)
1063.2(6)	7860	6796		$11/2^-$	$9/2^-$		
1109.5(5)	6454	5343		$11/2^+$	$9/2^+$	$M1+E2$	28(6)
1136.4(5)	4431	3295	0.69(2)	$7/2^-$	$5/2^+$	$E1$	207(26)
1218.2(5)	4634	3415	1.38(8)	$7/2^+$	$7/2^+$	$M1+E2$	43(18)
1266.4(5)	1266	0	1.0(1)	$3/2^+$	$1/2^+$	$M1+E2$	1000(163)
1338.6(6)	4634	3295	0.88(16)	$7/2^+$	$5/2^+$	$M1+E2$	30(7)
1442.7(8)	6080	4634		$9/2^+$	$7/2^+$	$M1+E2$	
1480.5(5)	6824	5343	0.63(11)	$11/2^-$	$9/2^+$	$E1$	156(14)
1511.4(6)	10217	8705		$15/2^-$	$13/2^-$		0.8(8)
1870.6(9)	9313	7442		$13/2^+$	$11/2^+$		
1880.8(5)	8705	6824		$13/2^-$	$11/2^-$	$M1+E2$	116(19)
1927.8(5)	5343	3415	0.76(2)	$9/2^+$	$7/2^+$	$M1+E2$	327(76)
2028.9(6)	3295	1266	1.17(4)	$5/2^+$	$3/2^+$	$M1+E2$	214(26)
2069.9(7)	6501	4431	1.62(14)	$9/2^-$	$7/2^-$	$M1+E2$	63(10)
2148.3(8)	3415	1266	1.26(3)	$7/2^+$	$3/2^+$	$E2$	664(84)
2197.9(9)	4431	2234		$7/2^-$	$5/2^+$	$E1$	293(45)
2204.2(9)	8705	6501		$13/2^-$	$9/2^-$		
2234.2(7)	2234	0		$5/2^+$	$1/2^+$	$E2$	658(68)
2358.0(10)	5773	3415		$(7/2^+)$	$7/2^+$		
2363.3(10)	6796	4431		$9/2^-$	$7/2^-$	$M1+E2$	56(9)
2393.6(7)	6824	4431		$11/2^-$	$7/2^-$	$E2$	
2860.6(12)	9313	6454		$13/2^+$	$11/2^+$	$M1+E2$	
3038.9(19)	6454	3415	1.44(5)	$11/2^+$	$7/2^+$	$E2$	214(62)
3232(3)	9313	6080		$13/2^+$	$9/2^+$		
3293.6(12)	3295	0		$5/2^+$	$1/2^+$	$E2$	
3381.6(16)	6796	3415		$9/2^-$	$7/2^+$		64(18)
3394.8(11)	10217	6824		$15/2^-$	$11/2^-$	$E2$	64(13)
3428.2(17)	7860	4431		$11/2^-$	$7/2^-$	$E2$	29(5)
3846(4)	6080	2234		$9/2^+$	$5/2^+$	$E2$	
4027(3)	7442	3415		$11/2^+$	$7/2^+$	$E2$	

et al. [18], on the other hand, populated states up to the energy of 13879 keV via the ^{24}Mg(^{16}O, $2\alpha 1p$) reaction with tentative spin-parity assignment of $(19/2^-)$ for this state. There are few discrepancies in both level schemes. First of all, the state proposed by Jenkins *et al.* [7] at 12171 keV was not confirmed in Ref. [18]. Furthermore, the negative parity of the 17/2 state at 11297 keV was not supported by the $M1+E2$ character of the 777-keV transition linking this state to the $15/2^+$ state at 10520 keV, as established in Ref. [18]. Importantly, the dipole character of the 2722-keV transition, deexciting the $13/2^-$ state at 9176 keV, unambiguously established in Ref. [18], sustained the negative parity of the state, contrary to the positive parity proposed in Ref. [7]. Finally, the $15/2^-$ assignment to the level at 10217 keV, due to firmly identified $E2$ and $M1+E2$ transitions to the $11/2^-$ at 6824 keV and $13/2^-$ at 9176 keV, respectively, is highly more probable than $J^\pi = 13/2^-$ proposed in Ref. [7]. This correction in the spin/parity assignment is important since it directly influences the MED values as discussed in the following sections. In the present work, excited states in ^{31}P were populated up to the $J^\pi = 15/2^-$ spin at 10217 keV. We report in Table I the observed transitions and, where the statistics allowed, the corresponding ADO ratios and relative intensities. The measured ADO ratios are in agreement with those of Ref. [18]. The resulting level scheme for ^{31}P is shown in Fig. 3, where a width of the arrows is proportional to the relative intensity of the transitions, corrected for the efficiency of the setup.

IV. LEVEL SCHEME OF ^{31}S

High spin states in ^{31}S were investigated previously in fusion-evaporation reactions. States up to the $J^\pi = 11/2^-$ spin at 6835-keV excitation energy were reported in Ref. [6] and up to the $J^\pi = (13/2^-)$ spin at 10146 keV in Ref. [7]. Both level schemes are in agreement. More recently, the

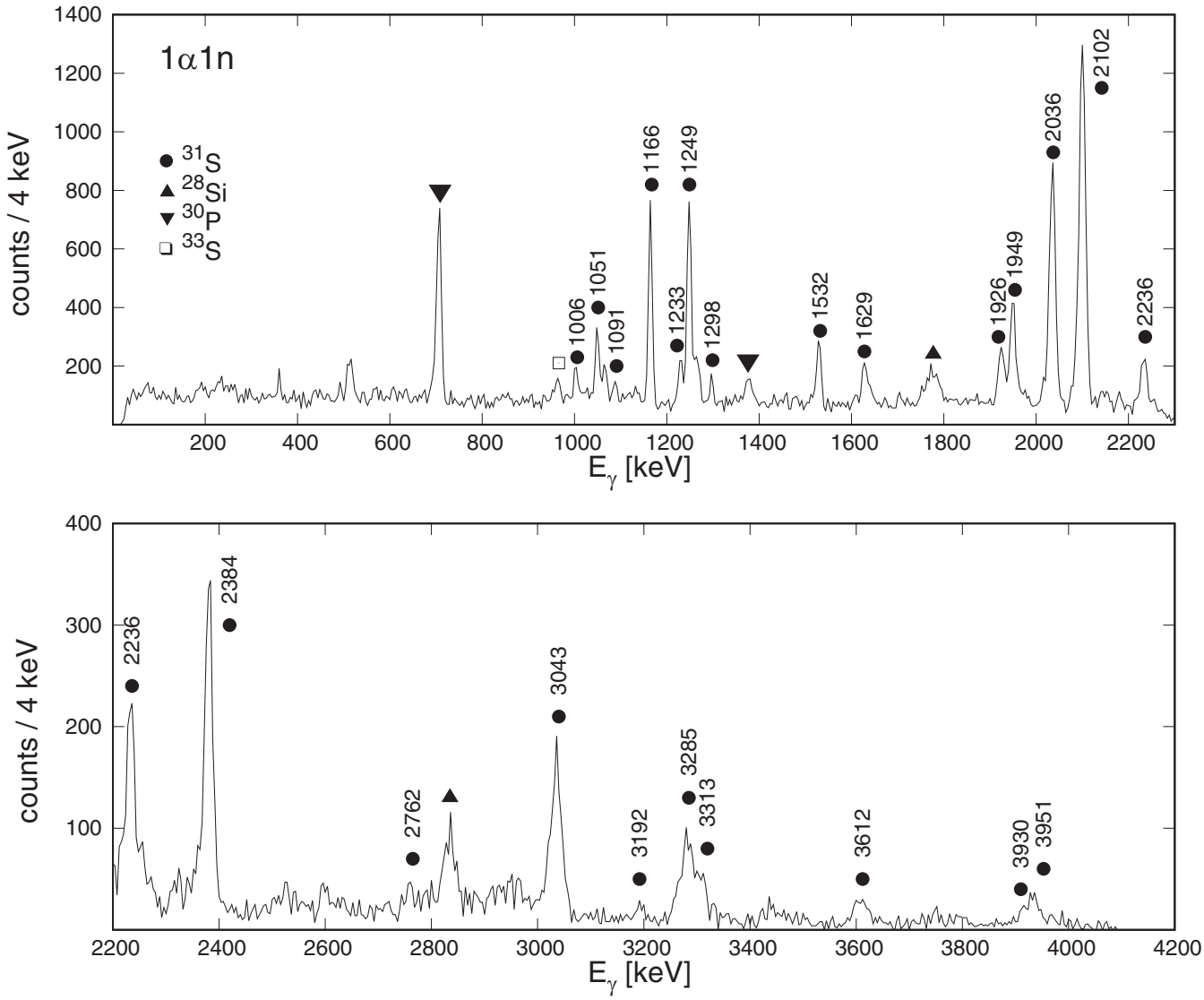

FIG. 2. Background-subtracted coincidence spectra obtained from E_γ-E_γ matrix using $1\alpha 1n$ condition and with a gate on γ-ray transitions of 1249 keV and 1166 keV.

structure of ^{31}S has been also studied in relation to the ^{30}P(p, γ)^{31}S reaction, which determines the material flux processed towards high-Z elements in nova environments (see Ref. [8] and references therein).

In the present work, excited states in ^{31}S were populated up to the $J^\pi = 13/2^+$ and $J^\pi = 15/2^-$ states at 9154 keV and 10146 keV excitation energy, respectively, see Fig. 2. The proposed level scheme, shown in Fig. 3, confirms the one reported in Refs. [6,7]. We have also observed the states at 5674 keV and 6636 keV assigned as $J^\pi = 7/2^+$ and $J^\pi = 9/2^-$ in Ref. [8]. A new state at 7642 keV, decaying by the 1006-keV and 3192-keV transitions, which were observed in coincidence with the 1166-keV, 1249-keV, and 2036-keV γ rays, was identified. The $J^\pi = 11/2^-$ spin was proposed as the mirror partner of the state at 7860 keV in ^{31}P. Two new γ-ray transitions of 3176 keV and 3743 keV were seen in coincidence with each other and with a transition of 2236 keV. Based on the state energy difference the transitions were tentatively attributed to deexcite the $13/2^+$ state at 9154 keV and the $(9/2^+)$ state at 5978 keV excitation energy. Based on mirror symmetry arguments, we assign $J^\pi = 15/2^-$ to the state at 10146 keV, as the isobaric analog of the 10217-keV state in ^{31}P, instead of the previous tentative attribution of $13/2^-$. In our analysis we have also observed transitions of 3612 keV and 3930 keV in coincidence with the 1249-keV, 2102-keV, and 2236-keV γ rays. However, as we cannot undoubtedly assign a position in the level scheme, they remain unplaced. Finally, the 2215 keV γ-ray transition linking the $7/2^-$ at 4451 keV with the $5/2^+$ at 2236 keV states, proposed in Ref. [7] can not be confirmed.

The observed transitions together with the corresponding R_{ADO} ratios and relative intensities, derived for the transitions with enough statistics, are reported in Table II. The

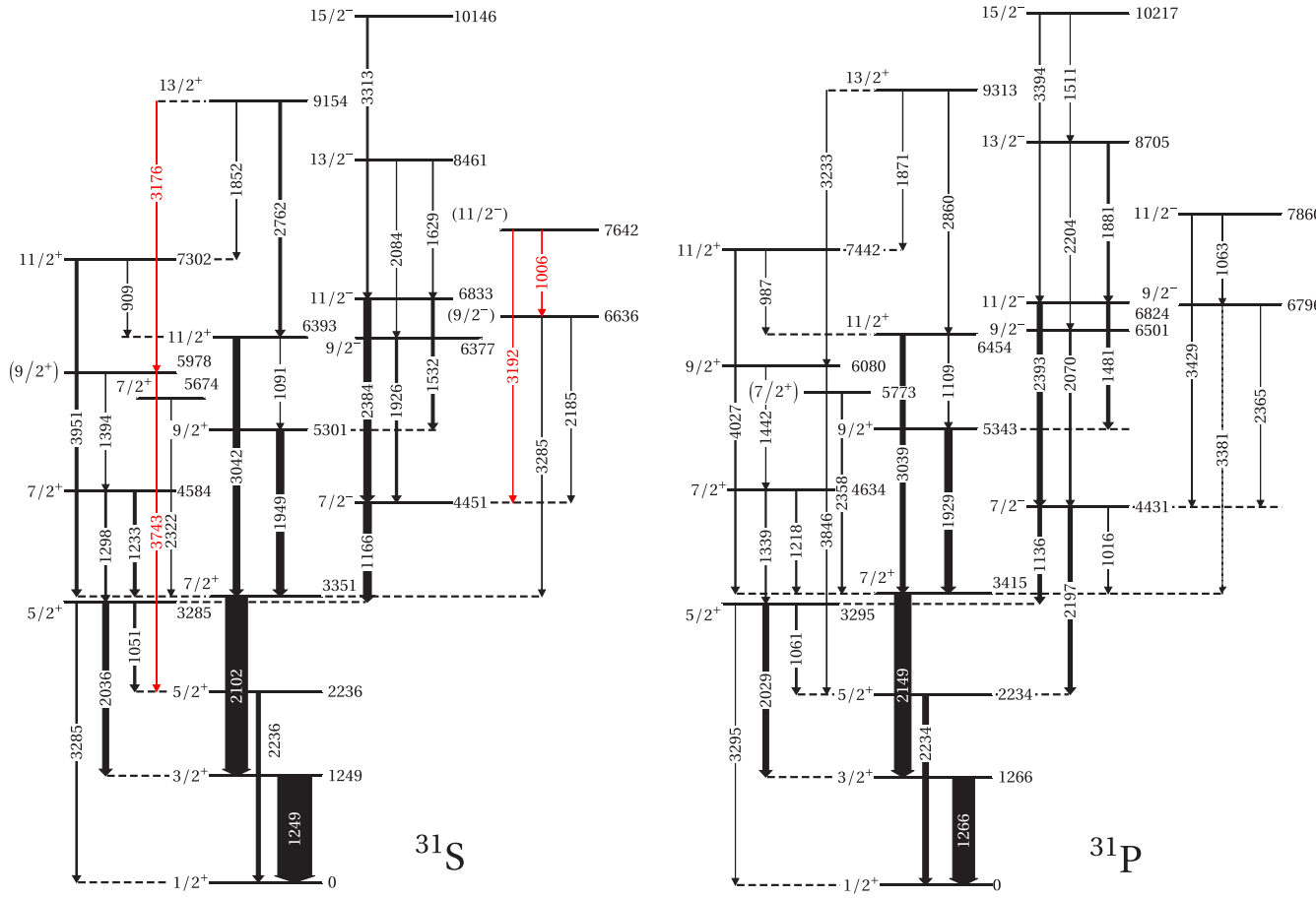

FIG. 3. Level schemes of ^{31}S and ^{31}P deduced from the present work. Newly observed transitions are in red.

resulting level scheme for ^{31}S is shown in Fig. 3, where a width of the arrows is proportional to the relative intensity of the transitions, corrected for the efficiency of the setup.

V. DISCUSSION

For the first time, we study here the structure of ^{31}S and ^{31}P in the shell model framework with a unique effective interaction that allows to describe both the positive- and negative-parity states. The isoscalar *psdpf* effective interaction of Ref. [19] has been developed in a large model space spanned by three main shells: *p*, *sd*, and *pf* and allows for one-particle–one-hole excitations between two main shells. Thus, the positive-parity states in the $A = 31$ mirror nuclei are described in the full *sd* shell while the negative-parity states are obtained by allowing only one nucleon to be excited from the *p* to the *sd* shell or from the *sd* to the *pf* shell.

We report in Fig. 4 the yrast states of ^{31}S for both parities in comparison with the calculated energies. The agreement is very good. From the analysis of the wave functions of the negative-parity states it results that these states are built by promoting one proton or one neutron, with almost equal probability, from the *sd* to the *pf* shell and, mainly, to the $f_{7/2}$ orbit. Excitations across $N = Z = 8$ result to be negligible.

To study the MED as a function of the angular momentum J we apply the method successfully developed for the nuclei in the $f_{7/2}$ shell [1,3], recently extended to nuclei in the *sd* shell [4]. The main contribution to the MED arises from the Coulomb interaction, which is separated in its multipole ($V_{\rm CM}$) and monopole contributions, and the isospin symmetry breaking term (V_B). The multipole Coulomb matrix elements are calculated in the harmonic oscillator basis within the whole valence space. Monopole contributions arise from the variation of the charge radius with the spin ($V_{{\rm Cr},J}$) and from single-particle energy corrections. The latter are due to the relativistic electromagnetic spin-orbit force (EMSO) $E_{\ell s}$ [5,20] and the orbit-orbit term $E_{\ell\ell}$ introduced in Ref. [21] to account for shell effects. The mirror energy difference for each analog state J is obtained, in the first order perturbation theory, by taking the difference of the expectation values of the various contributions between the mirror partners ($\Delta\langle V\rangle$):

$$\mathrm{MED}(J) = \Delta\langle V_{\rm CM}\rangle_J + \Delta\langle V_{\rm Cr}\rangle_J + \Delta(E_{\ell s} + E_{\ell\ell})_J + \Delta\langle V_B\rangle_J. \quad (2)$$

TABLE II. Transition energies for the observed γ-rays in ^{31}S along with the energy for the initial and final states, angular distribution ratio, multipolarity and the relative intensity.

E_γ	E_i	E_f					
keV			R_{ADO}	I_i	I_f	Mult.	I_γ^{rel}
907.6(5)	7302	6393		$11/2^+$	$11/2^+$	$M1+E2$[b]	
1006.1(5)[a]	7642	6636		$(11/2^-)$	$(9/2^-)$		
1051.4(3)	3285	2236	1.08(32)	$5/2^+$	$5/2^+$	$M1+E2$[b,d]	
1090.5(7)	6393	5301		$11/2^+$	$9/2^+$	$M1+E2$[b]	
1166.1(5)	4451	3285	0.82(2)	$7/2^-$	$5/2^+$	$E1$[b,c,d]	23(5)
1232.8(2)	4584	3351		$7/2^+$	$7/2^+$	$M1+E2$[b]	
1249.8(1)	1249	0	0.93(14)	$3/2^+$	$1/2^+$	$M1+E2$	100(12)
1298.4(3)	4584	3285	1.0(5)	$7/2^+$	$5/2^+$	$M1+E2$[b,d]	5(1)
1394.2(4)	5978	4584		$(9/2^+)$	$7/2^+$	$M1+E2$[b]	
1532.3(5)	6833	5301	0.81(25)	$11/2^-$	$9/2^+$	$E1$[b,c,d]	
1629.0(15)	8461	6833		$13/2^-$	$11/2^-$	$M1+E2$[b,d]	
1852.1(8)	9154	7302		$13/2^+$	$11/2^+$		
1926.4(8)	6377	4451	1.63(9)	$9/2^-$	$7/2^-$	$M1+E2$[b,d]	
1949.8(5)	5301	3351	0.64(15)	$9/2^+$	$7/2^+$	$M1+E2$[b,d]	
2035.9(8)	3285	1249		$5/2^+$	$3/2^+$	$M1+E2$	14(1)
2084.7(6)	8461	6377		$13/2^-$	$9/2^-$		
2101.9(5)	3351	1249	1.19(8)	$7/2^+$	$3/2^+$	$E2$[b,c]	60(7)
2184.4(20)	6636	4451		$(9/2^-)$	$7/2^-$	$M1+E2$[b]	
2235.8(8)	2236	0		$5/2^+$	$1/2^+$	$E2$	
2322.3(14)	5674	3351		$7/2^+$	$7/2^+$		
2384.3(8)	6833	4451	1.49(36)	$11/2^-$	$7/2^-$	$E2$[b,c,d]	
2761.7(30)	9154	6393		$13/2^+$	$11/2^+$	$M1+E2$[b,d]	
3042.2(10)	6393	3351	1.44(45)	$11/2^+$	$7/2^+$	$E2$[b,c,d]	
3176(3)[a]	9154	5978		$13/2^+$	$(9/2^+)$		
3192(6)[a]	7642[1]	4451		$(11/2^-)$	$7/2^-$	$E2$[b]	
3285.8(14)	3285	0		$5/2^+$	$1/2^+$	$E2$[b]	
3285.3(17)	6636	3351		$(9/2^-)$	$7/2^+$		
3313(4)	10146	6833		$15/2^-$	$11/2^-$	$E2$[b]	
3743(4)[a]	5978	2235		$(9/2^+)$	$5/2^+$		
3612(3)[a]		unplaced					
3930(3)[a]		unplaced					
3951(3)	7302	3351		$11/2^+$	$7/2^+$	$E2$[b,d]	

[a]newly observed transition.
[b]presently assigned multipolarity based on the mirror symmetry with ^{31}P.
[c]presently assigned multipolarity based on the measured ADO ratio.
[d]transitions for which DCO ratio was reported [7] but multipolarity assignment was not proposed; otherwise, the multipolarity is taken from the evaluation in Ref. [27].

The electromagnetic single particle corrections are obtained as:

$$E_{\ell s} = (g_s - g_\ell)\frac{1}{4m_N^2c^2}\left(\frac{-Ze^2}{R_C^3}\right)[j(j+1) - \ell(\ell+1) - s(s+1)], \quad (3)$$

where g_l and g_s are the g factors, m_N the nucleon mass, Z is the atomic number, R_C the charge radius. The EMSO contributes differently on protons and neutrons. This force, that has negligible effects in most of the MED studied in the $f_{7/2}$ shell, can give rise to large MED values of the order of 300 keV for particular configurations where a single nucleon, a proton in one nucleus and, consequently, a neutron in its mirror, is excited from the *sd* to the *fp* shell [23].

The $E_{\ell\ell}$ energy correction, of Coulomb origin, acts only on protons. It has been deduced in Ref. [21] and is given by

$$E_{\ell\ell} = \frac{-4.5Z_{cs}^{13/12}[2\ell(\ell+1) - N(N+3)]}{A^{1/3}(N+3/2)}\ \text{keV}, \quad (4)$$

with Z_{cs}, the atomic number of the closed shell and N the principal quantum number.

The nuclear radius depends on the occupation of the single orbitals. Protons in larger orbits feel less Coulomb repulsion and thus are more bound. Therefore, the change in the charge radius is computed by taking into account the change in the

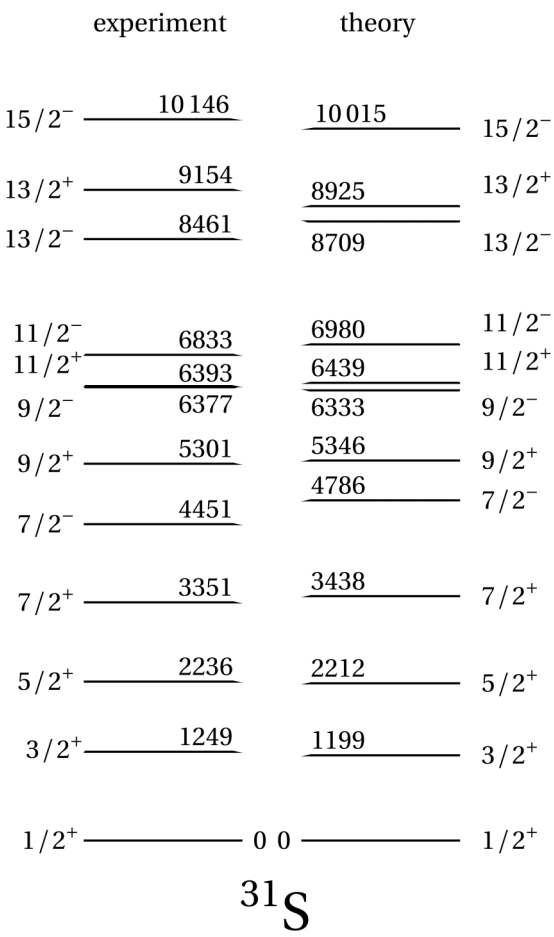

FIG. 4. Experimental and shell-model levels in ^{31}S.

occupation number of the orbits with larger radius as a function of the angular momentum. In a main shell, as it is the case of the *pf* shell in Refs. [2,3], low-ℓ orbits (*p* orbits) have larger radius than the high-ℓ ones (*f* orbits). In the *sd* shell, it is the *s* orbit that has larger radius than the *d* orbits [4,24]. Following Refs. [2–4], the radial contribution to the mirror energy differences is therefore obtained as the variation of the average proton (m_π) and neutron (m_ν) occupation numbers of the $s_{1/2}$ at angular momentum J with respect to the ground state (gs):

$$\Delta V_{\mathrm{Cr},J} = \alpha_r \left(\frac{(m_\pi(gs) + m_\nu(gs)}{2} - \frac{(m_\pi(J) + m_\nu(J)}{2} \right). \quad (5)$$

In Ref. [4] the α_r parameter was fixed at 200 keV, equal to that deduced in a systematic study of MED in nuclei of mass $A = 42$–54 [3]. In both cases, the low-ℓ orbits occupation number was less than one. Following Refs. [22,24] that show the reduction of the radius of the low-ℓ orbits when their occupation increases, we reduce the value of α_r to 100 keV for the $s_{1/2}$ shell. When describing the MED for negative parity states, we need to include in Eq. (5) also the contribution from the change in occupation number of the *f* and *p* orbits that have larger radii than the *d* orbits as well. We have used for these two orbits the α_r value of 200 keV. However, the radial contribution for these orbits is negligible and, therefore, differences of 50% in α_r does not influence significantly the results.

The ISB interaction V_B represents an additional term beyond the usual Coulomb interaction. It has been deduced from the mirror pair in mass $A = 42$ in Ref. [1], and recently extended to other main shells [4,25]. It consists on an isovector contribution with a difference of -100 keV between the proton-proton and neutron-neutron $J = 0$ matrix elements for all orbits. Its contribution to the MED values is not at all negligible as one should expect from isospin symmetry.

In Figs. 5(a) and 5(b) the experimental MED values for the positive-parity states are compared with the shell model results obtained with the code ANTOINE [26] using the effective *psdpf* interaction [19]. In Fig. 5(b) the contribution from the different terms in Eq. (2) are displayed. Overall, data are well described, except for the $5/2^+$ and $11/2^+$ states where 150 and 100 keV differences, respectively, with the experimental values are obtained. In Fig. 5(c), the MED corresponding to the negative-parity states are displayed, while the single contributions are reported in Fig. 5(d). The main contributions arise from the multipole Coulomb and the single-particle corrections $E_{\ell\ell} + E_{\ell s}$ terms. The electromagnetic spin-orbit term gives very large contribution ($\approx$300 keV) for pure single-particle excitations from the $d_{3/2}$ orbit to the $f_{7/2}$ one, as discussed above. Here, the excitation of a proton or a neutron have similar contributions, which compensates the effect. Still, the staggering trend reflects the fact that for the states $7/2^-$, $11/2^-$, and $15/2^-$ the probability of exciting a proton is larger than exciting a neutron across the $N = Z = 20$ gap in ^{31}P (the opposite in ^{31}S), while the probability is exchanged for the $9/2^-$ and $13/2^-$ states. Also the radial term V_{Cr} presents a staggering behavior. This is mainly due to the slightly larger occupation of the $s_{1/2}$ orbital by both protons and neutrons in the $9/2^-$ and $13/2^-$ states. Finally, the contribution of the ISB term for these states results relevant to improve the agreement with the data.

VI. CONCLUSIONS

The level scheme of ^{31}S has been extended and compared with the ^{31}P mirror partner, populated in the same experiment. This allowed the study of the behavior of the MED along the positive- and negative-parity yrast structures up to the spin $13/2^+$ and $15/2^-$, respectively. The level schemes were reproduced with good accuracy by means of shell model calculations in a large model space including three main shells with the *psdpf* interaction. The theoretical MED, calculated as a function of the angular momentum in both parity yrast sequences, describe very well the experimental data. The role of the different electromagnetic and ISB contributions has been discussed. Their behavior can be interpreted by analyzing the wave function configurations. In the present investigation we have used the same parametrization for the radial and ISB terms as the one adopted in our previous study for the $A = 23$ mirror pair [4]. Our new results, involving particle-hole excitations between two main shells, indicate that the method, originally deduced and successfully applied for $f_{7/2}$-shell nuclei can be successfully extended to nuclei in the *sd* shell including cross shell excitations.

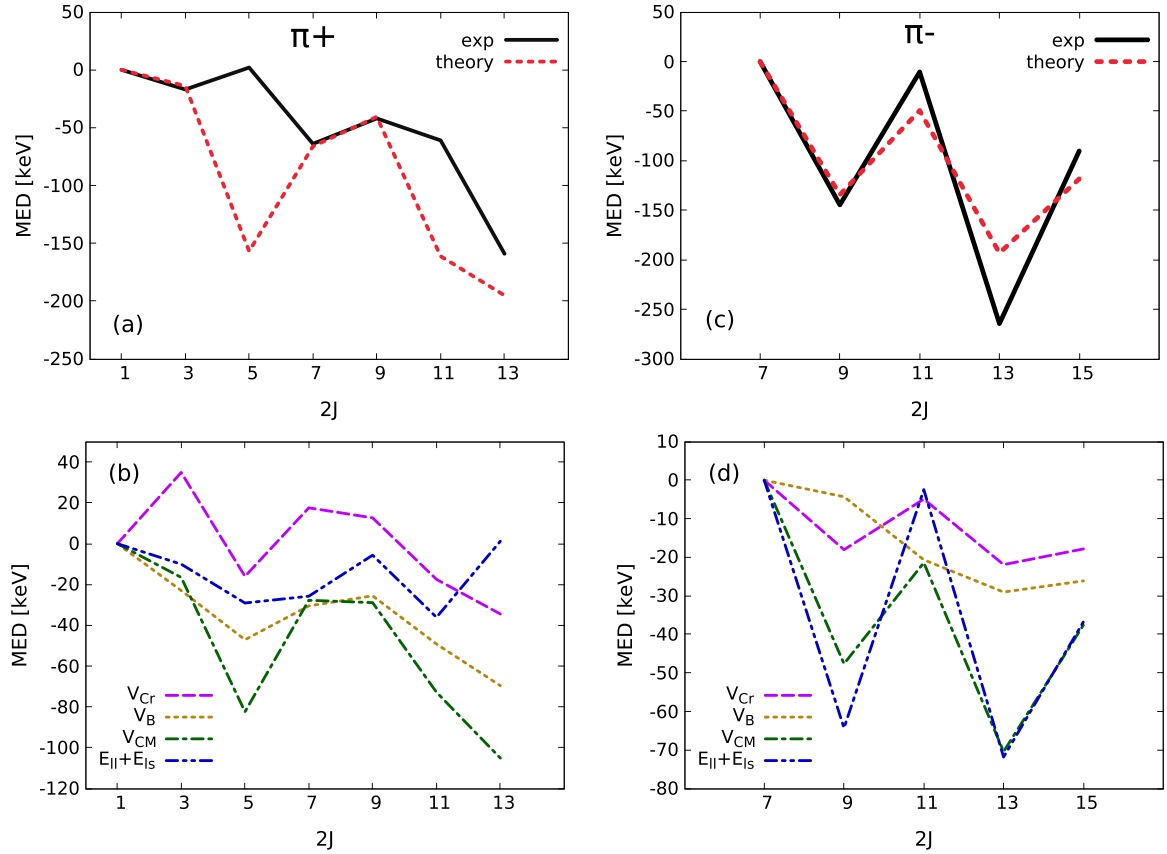

FIG. 5. Experimental MED for the states of (a) positive and (c) negative parity in $A = 31$ mirror nuclei compared with theoretical calculations: the radial contribution $V_{\rm Cr}$, the ISB term V_B, the multipole $V_{\rm CM}$ and the monopole $E_{\ell\ell} + E_{\ell s}$ terms to the resulting theoretical curve are plotted in (b) and (d).

ACKNOWLEDGMENTS

The authors would like to thank the technical staff of the LNL Legnaro facility for their assistance to provide excellent operation of the XTU-tandem accelerator. The authors also wish to acknowledge the support of the local engineers P. Cocconi and R. Isocrate. The work was supported by the National Science Centre, Poland (NCN) (Grant No. 2017/25/B/ST2/01569).

[1] A. P. Zuker, S. M. Lenzi, G. Martinez-Pinedo, and A. Poves, Phys. Rev. Lett. **89**, 142502 (2002).
[2] S. M. Lenzi *et al.*, Phys. Rev. Lett. **87**, 122501 (2001).
[3] M. A. Bentley and S. M. Lenzi, Prog. Part. Nucl. Phys. **59**, 497 (2007).
[4] A. Boso *et al.*, Phys. Rev. Lett. **121**, 032502 (2018).
[5] J. Ekman *et al.*, Phys. Rev. Lett. **92**, 132502 (2004).
[6] F. Della Vedova *et al.*, AIP Conf. Proc. **764**, 205 (2005).
[7] D. Jenkins *et al.*, Phys. Rev. C **72**, 031303(R) (2005).
[8] D. T. Doherty *et al.*, Phys. Rev. C **89**, 045804 (2014).
[9] C. Wrede, J. A. Caggiano, J. A. Clark, C. M. Deibel, A. Parikh, and P. D. Parker, Phys. Rev. C **79**, 045803 (2009).
[10] M. B. Bennet *et al.*, Phys. Rev. C **97**, 065803 (2018).
[11] A. Goasduff *et al.* (unpublished).
[12] D. Bazzacco, in *Workshop on Large γ-ray Detector Arrays No. AECL10613* (Chalk River Laboratories, Canada, 1992), p. 376.
[13] D. Testov *et al.*, Eur. Phys. J. A **55**, 47 (2019).
[14] J. Bradbury *et al.*, Nucl. Inst. Meth. A **979**, 164345 (2020).
[15] O. Skeppstedt *et al.*, Nucl. Instr. Meth. A **421**, 531 (1999).
[16] J. Ljungvall, M. Palacz, and J. Nyberg, Nucl. Instr. Meth. A **528**, 741 (2004).
[17] R. M. Steffen and K. Alder, in *The Electromagnetic Interaction in Nuclear Spectroscopy*, edited by W. D. Hamilton (North-Holland, Amsterdam, 1975).
[18] M. Ionescu-Bujor *et al.*, Phys. Rev. C **73**, 024310 (2006).
[19] M. Bouhelal, F. Haas, E. Caurier, F. Nowacki, and A. Bouldjedri, Nucl. Phys. A **864**, 113 (2011).
[20] J. A. Nolen and J. P. Schiffer, Annu. Rev. Nucl. Sci. **19**, 471 (1969).
[21] J. Duflo and A. P. Zuker, Phys. Rev. C **66**, 051304(R) (2002).

[22] J. Bonnard, S. M. Lenzi, and A. P. Zuker, Phys. Rev. Lett. **116**, 212501 (2016).
[23] S. Lenzi and R. Lau, J. Phys. Conf. S. **580**, 012028 (2015).
[24] J. Bonnard and A. P. Zuker, J. Phys. Conf. Ser. **1023**, 012016 (2018).
[25] M. A. Bentley, S. M. Lenzi, S. A. Simpson, and C. A. Diget, Phys. Rev. C **92**, 024310 (2015).
[26] E. Caurier and F. Nowacki, Acta Phys. Pol. B **30**, 705 (1999).
[27] C. Ouellet and B. Singh, Nucl. Data Sheets **114**, 209 (2013).